Coarse and fine combination technology based on gyrostability and missing target tracking

Yang Liu,[a,b,c] **Zhe An**,[d,*] **Yansong Song**,[b,c] **Yan Dong**,[e] **and Ye Gu**[b,c]

[a]Chinese Academy of Sciences, Changchun Institute of Optics, Precision Mechanics and Physics, Changchun, China

[b]Changchun University of Science and Technology, Key Laboratory of Fundamental Science on Space-Ground Laser Communication Technology, Changchun, China

[c]Changchun University of Science and Technology, School of Optoelectronic Engineering, Changchun, China

[d]Changchun Institute of Technology, School of Electrical and Information Engineering, Changchun, China

[e]Changchun University of Science and Technology, School of Electronic Information Engineering, Changchun, China

Abstract. High-precision, stable tracking technology on a mobile platform is a key technology for realizing the integration of airborne search and tracking. In this study, coarse-fine compound technology based on gyrostabilization and miss tracking is applied. First, the working principle of the coarse and fine composite system is analyzed, and then the coarse and fine composite algorithm is modeled. Thereafter, the error of the coarse and fine composite axis is analyzed, and the precision tracking servo control algorithm is designed. Finally, using the model and algorithm designed to control the single reflector and galvanometer, the coarse tracking of the space target and the fine tracking of the source are completed under the condition that the equivalent sine amplitude is 5 deg and the frequency is 0.2 Hz. At the same time, a test system was built for performance verification. The algorithm achieved a coarse-tracking azimuth-axis tracking accuracy [root mean square (RMS)] of 26.3 μrad and a pitch-axis tracking accuracy (RMS) of 28.9 μrad. After composite tracking was switched on, precision tracking azimuth-axis tracking accuracy (RMS) improved to 7.9 μrad and pitch-axis tracking accuracy (RMS) improved to 6.3 μrad, both better than 10 μrad. This study provides new insights into the stability and precision tracking of single cameras on airborne platforms. At the end of this work, the outdoor experiment to verify the influence of random interference on the system performance under given conditions and the subsequent optimization direction of the system are given. [DOI: 10.1117/1.OE.61.12.124104]

Keywords: airborne platform; servo control; coarse-fine compound; photoelectric tracking.

Paper 20220894G received Aug. 12, 2022; accepted for publication Nov. 21, 2022; published online Dec. 9, 2022.

1 Introduction

With the continuous development and optimization of devices and algorithms in recent years, the aviation and aerospace industry has been moving toward high speed, high precision, and high resolution.[1–3] Whether for laser communication on satellite platforms or stable imaging surveying and mapping on commercial aircraft, high-precision and high-reliability target tracking technologies are required as support mechanisms. Coarse and fine composite tracking technology is an effective way to achieve these goals. When the target source and load platform swing, the disturbance can be effectively suppressed, the target source can be locked, and stable, precise tracking can be achieved.[4,5]

*Address all correspondence to Zhe An, 2955100200@qq.com

0091-3286/2022/$28.00

This technology is widely used and can be applied to the acquisition, pointing, tracking (APT) subsystem of space laser communication, the tracking subsystem under the airborne platform, and the capture subsystem under the shipborne platform.[6–9] This study analyzes the airborne platform. Many organizations have conducted related research in this field. For example, OH-58D pod has precise tracking and night vision functions,[10] and a pod developed by Msis has high tracking accuracy and infrared detection capabilities.[11] Furthermore, China's University of Electronic Science and Technology is conducting an in-depth exploration of system design and theoretical analysis,[12] and China's Changchun University of Science and Technology has completed a 144-km communication verification experiment between two aircraft.[13] However, most of the aforementioned tracking systems, whether employing single-detector composite axis tracking or traditional dual-detector composite tracking, use miss tracking, that is, coarse tracking uses a two-dimensional turntable to achieve large-scale aiming, and the terminal uses galvanometers to achieve small-scale precision tracking.[14,15] The optical closed-loop feedback of the two actuators is provided by the camera, and this mode is mainly used on satellite platforms. For the airborne platform, only using miss distance tracking cannot effectively suppress the aircraft shaking and target disturbance during flight.[16–19] In addition, individual application scenarios are limited by the structure and weight of the mount, so there is no condition for using dual detectors or a single-detection composite axis optical path.[20–22] If only coarse tracking is used for tracking and aiming, the tracking accuracy is not high, which affects the application of the load function.[23]

This paper proposes a coarse and fine composite control technology based on gyrostabilization and miss tracking by modeling the system, analyzing the working principle, and designing coarse and fine tracking control models and control strategies. The system uses a camera to determine the miss distance for coarse tracking, and fine tracking uses gyroinformation and coarse-tracking residual information for further suppression, thereby achieving high-precision and stable tracking in the case of target source and load disturbances.[24–26] Finally, an experimental system was built for verification. The carrier was placed on a six-degree-of-freedom (DOF) rocking platform. The azimuth, pitch, and roll were controlled at 5 deg and 0.2 Hz to simulate the attitude changes of the aircraft during flight. The electromagnetic galvanometer was placed at the light source to simulate the standard vibration power spectrum. At this time, the root mean square (RMS) tracking accuracy of the coarse-tracking azimuth and pitch tracking was better than 30 μrad, and the RMS tracking accuracy of the fine tracking azimuth and pitch tracking was better than 10 μrad.

Although using a gyroscope or inertial navigation system on airborne or shipborne platforms has been common in recent years, most loads usually use a feedback closed-loop system to obtain high-precision tracking and aiming performance. Compared with other methods, on the one hand, in the coarse tracking branch, we introduce the inertial navigation feed-forward stabilization loop, solve the attitude motion of the carrier to the angle encoding axis with a tilt of 15 deg through coordinate transformation, and effectively compensate. On the basis of the feed-forward stabilization loop, a facula closed-loop is made, and the coarse tracking accuracy of the two axes under the moving platform is better than 30 μrad. On the other hand, in the fine tracking branch, different from the conventional method of using cameras as fine tracking feedback, we use inertial navigation information and coarse tracking residual information for suppression, inertial navigation information as the stability loop, and coarse tracking residual information as the real-time open-loop execution quantity. This method simplifies the fine tracking branch but requires a higher correction model. Because there is no optical miss distance as the feedback, it needs to have both a higher bandwidth and a smaller dynamic lag performance. With this method, we finally achieve a fine tracking accuracy better than 10 μrad under the moving platform.

2 Working Principle of Coarse and Fine Composite System

The coarse and fine composite system based on gyrostabilization and miss distance tracking is shown in Fig. 1. The system is composed of the following modules: master control, optical, image, detection, coarse tracking, and fine tracking. The image module completes target

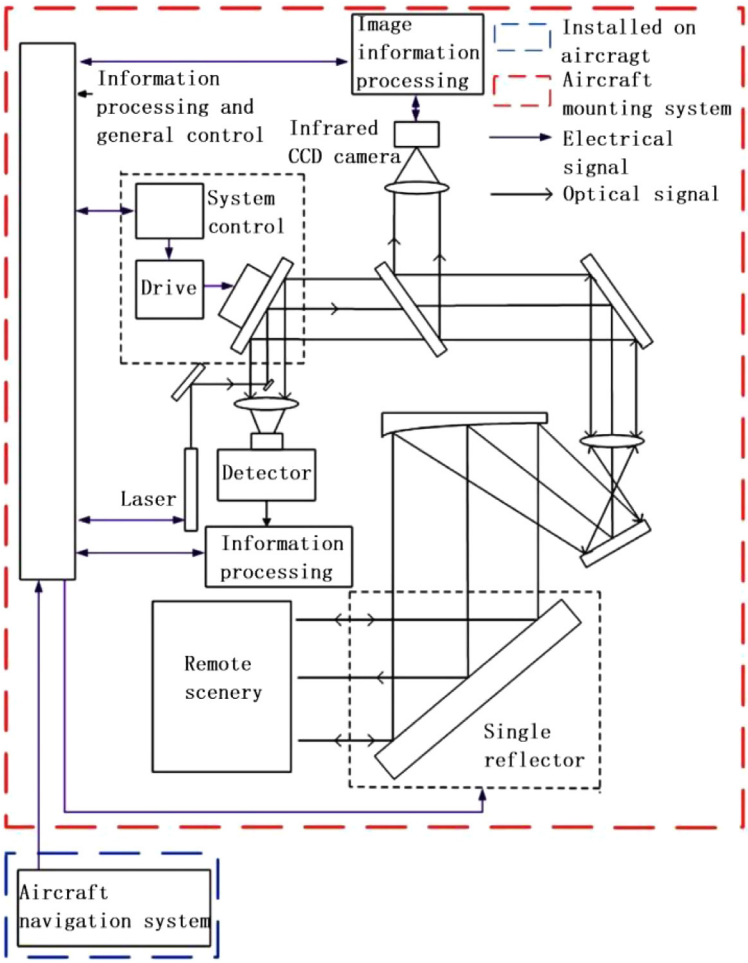

Fig. 1 Working block diagram of the coarse and fine composite system.

recognition and miss-target extraction, and feeds the information back to the coarse tracking module. The coarse-tracking module is composed of a single-lens reflex mirror and a control circuit. The coarse-fine composite actuator pulls the target into the coarse-tracking field of view and suppresses most of the disturbance. The precision tracking module consists of an electromagnetic galvanometer and a control circuit to complete the high-precision and stable tracking of the target. The optical module is composed of multiple reentrant mirrors that introduce the signal light into the working area. The detection module is composed of a camera, but it is used only to observe the tracking accuracy after the coarse and fine combination, and the miss amount of information is not returned to the tracking closed loop.

The single-lens reflex (SLR) and electromagnetic galvanometer in the system cooperate to complete the coarse and fine composite function. After the inertial navigation information is collected, the information processing module feeds back the speed information of the heading, pitch, and roll to the coarse-tracking and fine-tracking modules for algorithm processing. The miss distance is transmitted from the camera to the information acquisition module, and after processing, it is provided to the coarse-tracking module for the optical closed loop. The working principle of the coarse and fine composite is shown in Fig. 2. After coarse tracking and fine tracking respectively complete their own position closed loops, the camera and inertial navigation information are resolved to provide a position input for the dual control loop to complete the servo tracking. The tracking is turned on when the target source enters the field of view of the coarse-tracking camera. At this time, the coarse tracking is completed with the participation of the miss distance and the gyro. Then, the system enters the fine-tracking mode, and the fast mirror is used to further suppress the coarse-tracking residuals and complete the secondary composite tracking.

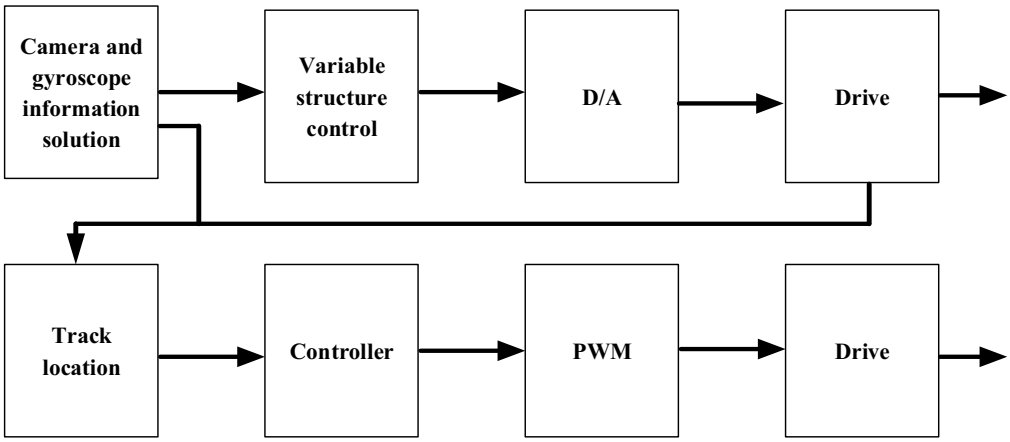

Fig. 2 Block diagram of the rough and fine composite working principle.

3 Design of Coarse-Fine Compound Control Strategy

3.1 *Coarse and Fine Composite Model Design*

The coarse stable-tracking loop has a larger stable range and lower servo bandwidth, which mainly realizes the initial stable tracking so that the target can reliably enter the range of the fine stable servo system. This system has a smaller dynamic range, higher servo bandwidth, and high stability accuracy. It effectively suppresses the coarse stabilization residual error and has a strong suppression ability for wide power spectrum vibration, ensuring a rapid rate, high precision, and high stability. The final stability accuracy of the compound tracking system depends on the performance of the fine stability servo unit.

The work of the system can be divided into two stages. The first stage is coarse stabilization tracking. The system miss amount is input into the rough stabilization loop by the gyrosensor and image miss amount. Then the SLR mirror is driven to suppress the platform attitude change, and the target is introduced into the fine tracking adjustment range to achieve the purpose of initial stable tracking. The second stage is fine and stable tracking. The position information is calculated by the inertial navigation and tracking residuals. The the fine tracking loop controls the fast mirror to complete the fine correction of the sight axis to achieve the goal of stable target tracking. The composite control model is shown in Fig. 3.[27]

In Fig. 3, $E_{\text{main}}(s)$ and $E_{\text{aux}}(s)$ are the output characteristic function of the sensor. $D_{\text{main}}(s)$, $G_{\text{main}}(s)$, $D_{\text{aux}}(s)$, and $G_{\text{aux}}(s)$ are the controller and transfer function of the coarse and fine tracking system, respectively. From Fig. 3, the equivalent closed-loop transfer function of the system is obtained as follows:

$$W(s) = \frac{C(s)}{R(s)} = \frac{W_{\text{main}}(s) + W_{\text{aux}}(s) + W_{\text{main}}(s)W_{\text{aux}}(s)}{[1 + W_{\text{main}}(s)][1 + W_{\text{aux}}(s)]}. \tag{1}$$

In the equation, $W_{\text{main}}(s) = E_{\text{main}}(s)D_{\text{main}}(s)G_{\text{main}}(s)$ and $W_{\text{aux}}(s) = E_{\text{aux}}(s)D_{\text{aux}}(s)G_{\text{aux}}(s)$. The open-loop transfer function is obtained as follows:

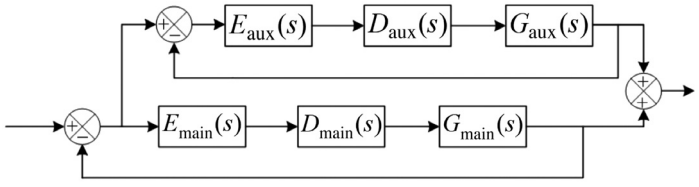

Fig. 3 Compound control model.

$$W_{\text{open}}(s) = W_{\text{main}}(s) + W_{\text{aux}}(s) + W_{\text{main}}(s)W_{\text{aux}}(s). \tag{2}$$

Regardless of noise, the error transfer function derived from Eq. (2) is shown in Eq. (3) as follows:

$$W_e(s) = 1 - W(s) = \frac{1}{[1 + W_{\text{main}}(s)][1 + W_{\text{aux}}(s)]}. \tag{3}$$

Analyzing the models of the equations given above, we can observe that the composite axis in the low frequency band approximates the main axis and slave axis in series, and the transfer function is a multiplication relationship. The magnification factor is much larger than that of the single-spindle system, and it has a high static error suppression capability. In the middle- and high-frequency bands, the composite shaft is approximately equal to the slave shaft system, which has a higher bandwidth and dynamic error suppression capability. Therefore, using this coarse-fine composite model can enable large-scale, high-precision, stable tracking.

3.2 *Error Analysis of Coarse and Fine Composite Shaft*

In the coarse and fine composite axis control system, when the main shaft circuit is not stable, the slave axis does not function.[28,29] At this time, the stability error depends entirely on the main shaft, which is equivalent to the single coarse-tracking working state. After entering the composite shaft to work, Eq. (3) shows that the error transfer function is the product of the master-and-slave system error transfer functions, and the system error is approximately equal to the stable error of the slave shaft. The noise factor is not considered in Eq. (3), but in the actual work process, detector noise and external random interference are introduced into the system, so a composite axis control system with added noise is designed, as shown in Fig. 4.

The error transfer functions of the master and slave axes after introducing noise are shown in the following equations:

$$W_{\text{emain}}(s) = \frac{E_{\text{emain}}(s)}{R_{\text{main}}(s)} = \frac{1 + \frac{N_{\text{main}}}{R_{\text{main}}}}{1 + W_{\text{main}}}, \tag{4}$$

$$W_{\text{eaux}}(s) = \frac{E_{\text{eaux}}(s)}{R_{\text{aux}}(s)} = \frac{1 + \frac{N_{\text{aux}}}{R_{\text{aux}}}}{1 + W_{\text{aux}}}. \tag{5}$$

Derived from Eqs. (4) and (5), the total error transfer equation is as follows:

$$W_e(s) = \frac{\left[1 + \frac{N_{\text{main}}(s)}{R_{\text{main}}(s)}\right]\left[1 + \frac{N_{\text{aux}}(s)}{R_{\text{aux}}(s)}\right]}{[1 + W_{\text{main}}(s)][1 + W_{\text{aux}}(s)]}, \tag{6}$$

where $N_{\text{main}}(s)$ represents the input noise signal of the main shaft and $N_{\text{aux}}(s)$ represents the input noise signal of the slave shaft, both of which contain inertial navigation output error information. $R_{\text{main}}(s)$ and $R_{\text{aux}}(s)$ are the input signals of the master and slave axis, respectively. When the noise is negligible relative to the input, Eqs. (3) and (6) are equivalent. When the Gaussian distributed white noise is introduced, as the noise increases, the effective suppression range of the error decreases, which affects the stability of the system. In general, the stability of

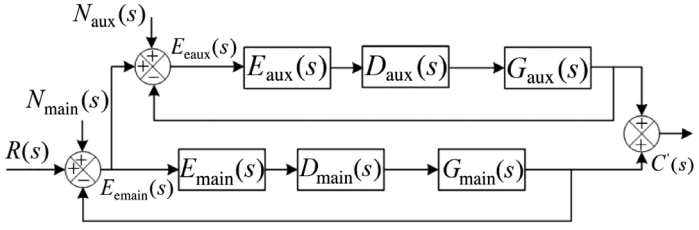

Fig. 4 Compound shaft control system with noise.

the system depends on the mid-frequency band of equivalent open-loop characteristics. In a coarse-fine composite system, the greater the high-frequency attenuation of the master axis is, the greater the contribution to the stability of the slave axis is. The high-frequency noise of the spindle residual directly affects the stability accuracy of the slave axis, especially when the coarse and fine bandwidths are small, that is, the zero-crossing peak value of the amplitude-frequency characteristic curve of the error transfer function of the two axes is close. At this time, the noise signal is amplified to a certain extent, thereby reducing the system stability. During the period when the coarse tracking does not enter stable tracking, the fine tracking does not work. Therefore, the prerequisite of the coarse and fine composite system is that the coarse tracking must be stable first. After stabilization, the higher the precision of tracking is, the smaller the total system error of the composite axis is, and the better the suppression of tracking noise is.

3.3 *Precision Tracking Servo Control Design*

The original system is often unstable under the condition of the total open-loop gain determined according to the steady-state design or lacks sufficient stability margin to make the transient response performance of the system very poor. At this time, a suitable series compensator must be introduced into the original system to fundamentally improve the quality of the original system. The design process of fine tracking adaptive compensation based on the Bode diagram is as follows. First, the desired open-loop logarithmic frequency characteristics of the system must be established according to the steady-state and transient performance of the system. Then, the open-loop logarithmic frequency characteristic of the original system is established, so the total open-loop gain is determined by the steady-state design. Then, a compensator to modify the open-loop logarithmic frequency characteristic of the original system is introduced to make it approach the desired open-loop logarithmic frequency characteristic. The result of subtracting the ordinate of the open-loop logarithmic amplitude frequency characteristic and the original system's open-loop logarithmic amplitude frequency characteristic provides the logarithmic amplitude frequency characteristic of the series compensator. Finally, its corresponding transfer function can be directly determined by the logarithmic amplitude frequency characteristics of the compensator, and it can be realized by analog or digital technology.

The Bode diagram design method is an inside-out design method. The performance of the closed-loop system is obtained by designing the desired open-loop logarithmic frequency characteristic, and the result is not necessarily completely expected. This is because of the difficulty in expressing the relationship between the open-loop logarithmic frequency characteristic parameters and the closed-loop system performance parameters of a high-order system with strict and accurate mathematical formulas, and this relationship can only be expressed by approximate engineering equations. Therefore, Bode design results often need to be revised iteratively. In the design of the precision tracking system, the adaptive characteristics are mainly reflected in the design process of the mid-frequency band. The shape of the mid-frequency band basically determines the dynamic performance of the control system. It is mainly reflected in the relationship between the system bandwidth ω_B and the open-loop cutoff frequency ω_c, as well as the amplitude frequency characteristic peak value $M_{p\omega}$ and the phase angle margin γ. According to the specific relationship between them, when the system frequency domain requirements are given, the open-loop cutoff frequency ω_c can be determined. In general, -20 dB/dec is expected to be used to pass through the mid-frequency band, as shown in Fig. 5.

To facilitate the design, a new variable h is introduced, and $h = \omega_3/\omega_2 = T_2/T_3$ represents the length of the mid-band of -20 dB/dec. When h is determined, the open-loop model of the system is simplified, and the following equation is obtained:

$$W_{\mathrm{p}\omega} = \frac{h+1}{h-1}, \quad h = \frac{M_{\mathrm{p}\omega}+1}{M_{\mathrm{p}\omega}-1}. \tag{7}$$

Furthermore, ω_2, ω_3, and ω_{c} are obtained to satisfy the best proportional relationship as follows:

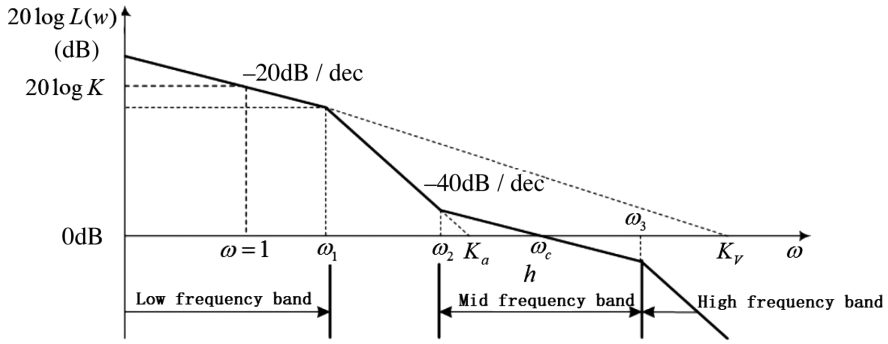

Fig. 5 Open-loop amplitude frequency characteristic curve of the control system.

$$\frac{\omega_3}{\omega_c}=\frac{\omega_3}{\omega_r}\cdot\frac{\omega_r}{\omega_c}=\sqrt{h}\frac{2\sqrt{h}}{h+1},\quad \frac{\omega_2}{\omega_c}=\frac{\omega_2}{\omega_3}\cdot\frac{\omega_3}{\omega_c}=\frac{2}{h+1}. \tag{8}$$

In the equation, ω_r represents the resonant frequency of the system. The frequency band of the system designed according to Eq. (8) can minimize $M_{p\omega}$ and obtain the best relative stability. The characteristic curve of $M_{p\omega}$ with h is shown in Fig. 6.

Analyzing Fig. 6, we can observe that when h is small, $M_{p\omega}$ changes drastically with h. When $h > 10$, $M_{p\omega}$ does not change significantly with h. When h is further increased, the system performance is not greatly improved. Therefore, in combination with application requirements, h is set as a value of 6, where $M_{p\omega} = 1.4$, $\omega_2/\omega_c = 0.29$, and $\omega_3/\omega_c = 1.71$. According to the preceding parameters, the correction and compensation function of the design system are given as shown in the following equation:

$$D(s)=\frac{K\left(1+\frac{1}{\omega_2}s\right)\left(1+\frac{1}{\omega_3}s\right)}{s\left(1+\frac{1}{\omega_1}s\right)\left(1+\frac{1}{\omega_4}s\right)}=\frac{1.8\times10^4\left(1+\frac{1}{60}s\right)\left(1+\frac{1}{750}s\right)}{s\left(1+\frac{1}{5}s\right)\left(1+\frac{1}{1000}s\right)}. \tag{9}$$

The characteristic curve drawn according to the correction function is shown in Fig. 7. The phase angle margin of the system is 44.8 deg, and the system is stable. As fine tracking is a digital control system, Eq. (9) should be discretized, and the discretized compensation function is shown as follows:

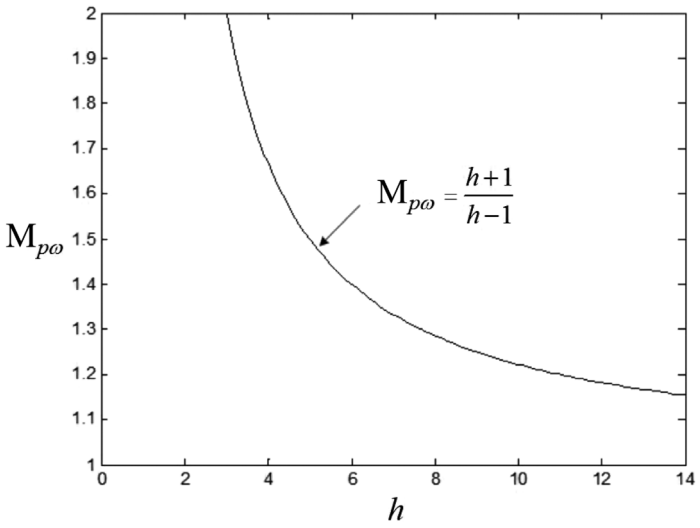

Fig. 6 $M_{p\omega}$ and h relation curve.

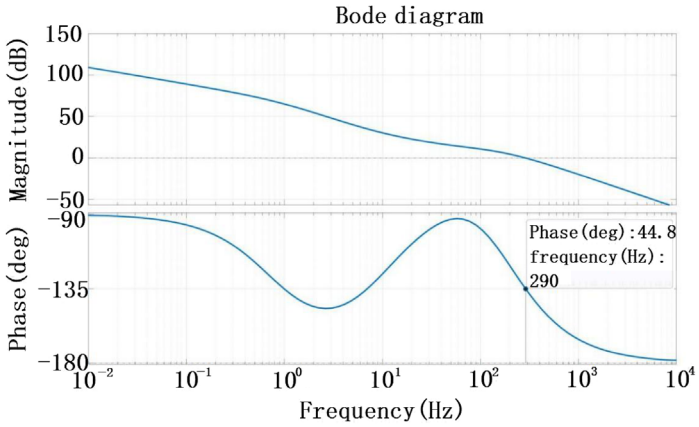

Fig. 7 Open-loop amplitude frequency characteristic curve of the fine tracking variable structure servo system.

$$D(z) = \frac{0.6477z^{-1} - 1.14z^{-2} + 0.4947z^{-3}}{1 - 2.715z^{-1} + 2.43z^{-2} - 0.7153z^{-3}}. \tag{10}$$

After simplifying the preceding formula, the transfer function of the APT precision tracking digital control compensator is

$$\begin{aligned} y(0) = {} & 0.6477x(-1) - 1.14x(-2) + 0.4947x(-3) \\ & + 2.715y(-1) - 2.43y(-2) + 0.7153y(-3). \end{aligned} \tag{11}$$

4 Coarse and Fine Composite Performance Test Based on Miss Distance and Inertial Navigation Tracking

To verify the performance of the coarse and fine composite system based on gyrostability and miss tracking, an experimental system, as shown in Fig. 8, was built. The system includes two cameras: camera 2 provides the amount of miss for coarse tracking and camera 1 only observes the state of fine tracking and does not feed back any signal for the closed loop. The optical system refracts light back into the camera. The light source provides a stable target signal.

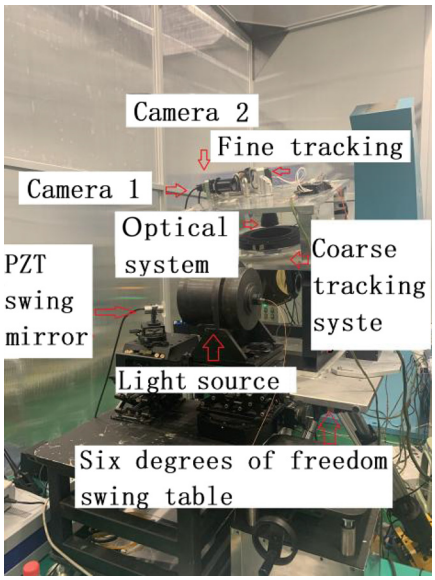

Fig. 8 Coarse-fine composite test system.

The piezoelectric ceramic transducer (PZT) swing mirror changes the optical path and simulates the vibration of the target source. The 6-DOF swing platform simulates the disturbance of the aircraft platform. Coarse and fine tracking systems are the implementing agencies of the coarse and fine compound algorithm. The electric control box is used to run the designed control algorithm and realize the corresponding function. The inertial navigation provides the solution information of the platform attitude swing for the composite system and participates in the closed loop of the algorithm.

The straight-line positioning accuracy of the 6-DOF swing table is better than ± 0.02 mm, and the attitude angle positioning accuracy is better than ± 0.01 deg. The angular resolution of the PZT swing mirror in the experimental system is better than 5 μrad, the 3-dB bandwidth is better than 1000 Hz, the step response time of 1 mrad is <5 ms, and the repeated positioning accuracy is 1%. In the tracking and aiming system, the heading angle alignment accuracy of inertial navigation system (INS) is better than 0.3 deg, the attitude angle alignment accuracy is better than 0.05 deg, and the heading angle and attitude angle retention accuracy are better than 0.1 deg. In the system, the angular velocity zero position repetition accuracy of the gyroscope is <0.05 deg /h, the angular velocity zero position stability accuracy is <0.05 deg /h, and the angular velocity linearity is better than 200 ppm.

When verifying the performance of the coarse and fine composite system, the light emitted by the light source is refracted into the system by the PZT pendulum mirror, and the pendulum mirror simulates the movement state of the target source with the standard vibration power spectrum. The refracted light enters the optical system through the coarse-tracking system and camera 2 imaging. The miss distance information is transmitted back to the coarse tracking to form an optical closed loop. At the same time, the 6-DOF rocking platform swings azimuth, pitch, and roll with parameters of amplitude ± 5 deg and frequency 0.2 Hz to simulate the vibration curve of the airborne platform. The equivalent sine with amplitude of 5 deg and frequency of 0.2 Hz can simulate the angular velocity of 6.28 deg/s and the angular acceleration of 7.9 deg $/s^2$. The inertial navigation is sensitive to the three-axis motion attitude and sends the information back to the coarse and fine tracking systems to make a closed loop. The frame rate of cameras 1 and 2 is set to 200 Hz, the angular resolution of camera 2 is 16.9 μrad/pixel, and the angular resolution of camera 1 is 3.46 μrad/pixel. The angular resolution here is determined by the field of view and focal length, and its size will also affect the tracking accuracy. We know that the definition of angular resolution is the radian value of a unit pixel. Because the optical closed-loop system uses the miss distance as the feedback value and its unit is a pixel, except for the dynamic lag error, the tracking accuracy can never be less than that of a unit pixel. Therefore, from this perspective, the smaller the angular resolution is, the better the accuracy is. However, if you want to maintain a smaller angular resolution, you need a larger focal length and a smaller field of view. A smaller field of view is not conducive to the capture of light spots. Therefore, the selection of angular resolution is a process of optimal selection. The angle resolution of camera 1 and camera 2 is the parameter after optimization. For the coarse tracking branch, we choose the pixel size of 15 μm, the field of view specification is 512×512, and the focal length is 887 mm. This not only meets the requirements of remote target detection but also ensures that the branch has a high angular resolution. For the fine tracking branch, we choose the pixel size of 15 μm, the field of view specification is 376×376, and the focal length is 4335 mm. This design not only ensures that the coarse heel residual is in the fine tracking field of view but also further improves the angular resolution. After fine tracking is turned on, the miss distance information of observation camera 1 is uploaded to the master control of the upper computer for RMS statistics to obtain the composite tracking accuracy. Figure 9(a) shows the tracking residual curve of the coarse-tracking system, and Fig. 9(b) shows the composite tracking residual curve after the participation of fine tracking. The miss curve in Fig. 9(a) has obvious periodic characteristics, which is due to the periodic motion of the 6-DOF swing table. The algorithm that we designed mainly aims to verify the suppression effect under the conditions that the maximum angular velocity does not exceed 6.28 deg/s and the maximum angular acceleration does not exceed 7.9 deg $/s^2$. Therefore, we give an equivalent sine amplitude of 5 deg and a frequency of 0.2 Hz to simulate the attitude disturbance. Our 6-DOF swing platform is limited by its own performance and cannot meet the designed maximum angular velocity and maximum angular acceleration under random disturbance conditions. Therefore, we plan to carry out a unmanned aerial vehicle (UAV) hook up test at

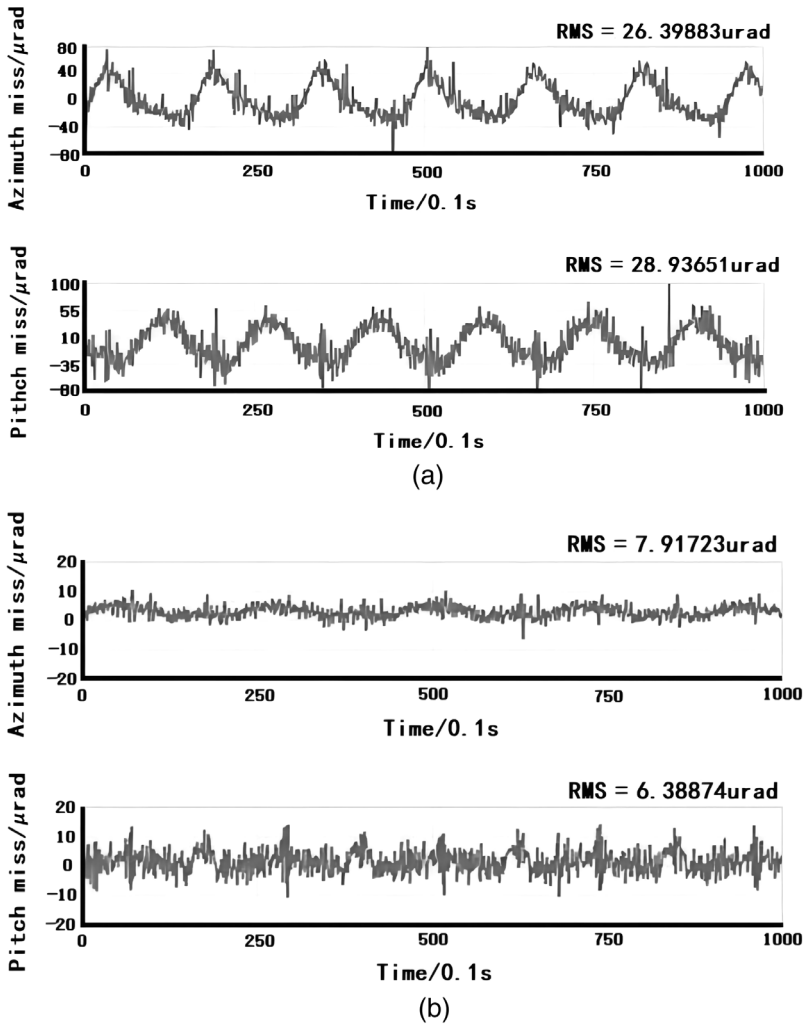

Fig. 9 (a) Rough tracking residual curve and (b) composite tracking residual curve.

the end of the year, and the UAV will be used as a random disturbance platform to verify the performance of the composite control strategy.

Through the test curve, we found that, using the tracking control model designed in this paper, the tracking accuracy RMS of the coarse-tracking azimuth axis is 26.3 μrad, and the tracking accuracy RMS of the coarse-tracking pitch axis is 28.9 μrad, both of which are better than 30 μrad. The reason for achieving this high-performance rough tracking is that, in terms of control strategy, we use double closed-loop tracking and an inertial navigation feedforward stabilization loop to suppress the attitude disturbance at the first level; then we use the camera output miss distance as the feedback signal to build an optical closed-loop loop to suppress the residual error at the second level. In terms of the control algorithm, after optimizing the model and control parameters, we not only make the rough tracking loop have better dynamic performance but also make the loop have a higher tracking bandwidth. In terms of device selection, to ensure the real-time dynamic performance, we choose an inertial navigation with an output frame rate of 1000 Hz and a camera with an output frame rate of 100 Hz. To match the frequency of peripherals, we increase the control frequency to 1000 Hz. After the composite tracking is turned on, the azimuth axis tracking accuracy RMS is 7.9 μrad, and the pitch axis tracking accuracy RMS is 6.3 μrad, both of which are better than 10 μrad. After coarse fine composite tracking, the remaining tracking error is mainly composed of the angular resolution error of the camera, the dynamic lag error of the compensation algorithm, and the systematic error of the optical mechanical installation. The dynamic lag error is determined by the stability and alignment accuracy of inertial navigation system, the suppression accuracy of tracking algorithm

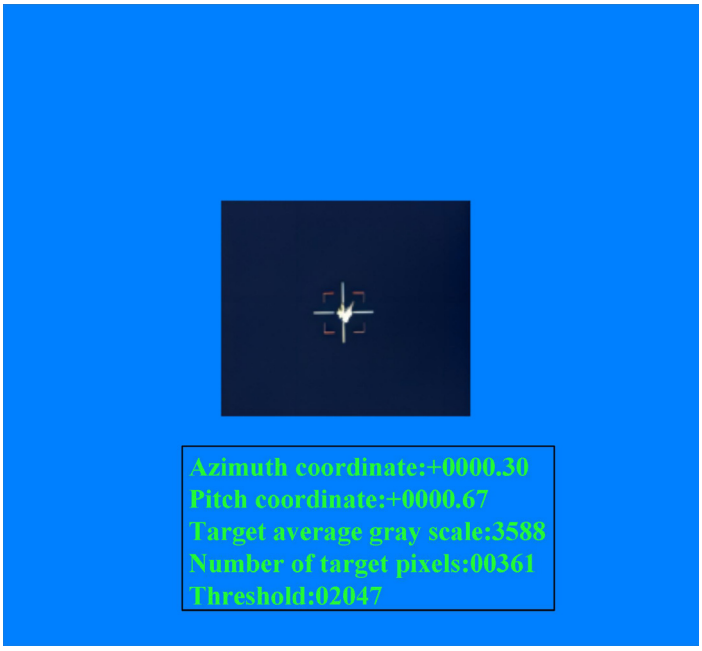

Fig. 10 Miss distance of coarse-fine compound tracking.

under low-frequency disturbance, and the frame frequency of the miss distance feedback. From the existing experimental conditions and peripheral performance, it has reached a good tracking state. To further improve the tracking accuracy of 10 μrad of the system, the next step is to optimize the algorithm and improve the performance of the device. This will be the focus of future research.

Then, we use conventional control algorithms and do not introduce gyrodata for the closed loop. The experiment shows that the coarse-tracking azimuth RMS is 29.7 μrad, the pitch RMS is 33.2 μrad, the fine tracking azimuth RMS is 17.3 μrad, and the pitch RMS is 21.6 μrad. The light spot after the coarse and fine composite tracking is stable is shown in Fig. 10. Comparing the experimental data, we find that the use of the gyrostabilized variable structure servo correction algorithm does not significantly improve the coarse-tracking accuracy, but it improves the fine-tracking accuracy more significantly. Coarse tracking has optical closed-loop and self-closed-loop locking, which is more effective for the disturbance suppression of the platform. However, as the fine tracking does not lock the miss distance, it only corrects the coarse tracking residuals from time to time. Therefore, the introduction of the gyrostabilized closed loop can suppress the platform vibration more effectively and improve tracking accuracy. The above experimental conclusions are obtained from many experiments, and the RMS value of multiple groups of data is taken as the tracking accuracy in a single experiment. Therefore, it has not only good repeatability but also a certain persuasiveness in evaluating the system performance.

5 Conclusion

We modeled the coarse and fine compound technology based on gyrostabilization and miss tracking and designed the coarse and fine compound strategy, including model design, axis error analysis, and fine tracking servo control design. In the case of double perturbation, high precision, stable composite tracking is realized without extracting the miss distance from the precision tracking. Finally, an experimental system was built for verification. When the 6-DOF rocking table is perturbed by a ± 5 deg, 0.2 Hz spectral line and the PZT galvanometer is vibrating with the standard vibration power spectrum, the coarse and fine composite tracking test is completed. The experimental results show that the designed control strategy and control algorithm significantly improve the precision of the coarse and fine composite tracking. The coarse-tracking azimuth axis tracking accuracy RMS is 26.3 μrad, pitch-axis tracking accuracy RMS is

28.9 μrad, fine-tracking azimuth axis tracking accuracy RMS is 7.9 μrad, and pitch-axis tracking accuracy is RMS. The accuracy RMS is 6.3 μrad. After the composite tracking is switched on, the dual-axis tracking accuracy is better than 10 μrad. The servo control model designed in the study has completed the initial laboratory verification and provides a new idea for the stable and precise tracking of a single camera under the airborne platform. At the same time, it provides a reference for the search and follow integration technology under the airborne platform.

At this stage, we have completed the system integration and demonstration verification in the laboratory. Limited by the indoor conditions, we have not verified the performance of our system and algorithm on a random disturbance platform and can only replace it with the equivalent sinusoidal motion of the 6-DOF swing platform. In the next stage, we will conduct outfield demonstration and verification. It is expected that the system will be loaded on the UAV platform at the end of the year. At that time, the UAV will fly with the maximum angular velocity of 6.28 deg/s and angular acceleration of 7.9 deg $/s^2$. The aircraft attitude swing during flight will be a random signal to verify the impact of random interference on system performance under given conditions. At the same time, we will further develop models and algorithms so that the servo algorithm can track real images in real scenes.

Acknowledgments

Natural Fund Project of Science and Technology Department of Jilin Province (Grant No. YDZJ202101ZYTS193).

References

1. Y. Cao et al., "Research on high precision permanent magnet servo control system of airborne stable platform," in *IEEE 5th Inf. Technol. and Mechatron. Eng. Conf. (ITOEC)* (2020).
2. F. Wang et al., "Stabilization control mothed for two-axis inertially stabilized platform based on active disturbance rejection control with noise reduction disturbance observer," *IEEE Access* **7**, 99521–99529 (2019).
3. H. Li, "Limited magnitude calculation method and optics detection performance in a photoelectric tracking system," *Appl. Opt.* **54**(7), 1612–1617 (2015).
4. G. Wang, Y. G. Guo, and S. J. Zhang, "Physical simulation of trajectory tracking for tracking performance evaluation of photoelectric turntable," *Optoelectron. Lett.* **16**(4), 272–278 (2020).
5. M. Xie et al., "Application research of high-precision laser beam pointing technology in airborne aiming pod," *Optik* **183**, 775–782 (2019).
6. R. Opromolla, G. Inchingolo, and G. Fasano, "Airborne visual detection and tracking of cooperative UAVs exploiting deep learning," *Sensors* **19**(19), 4332 (2019).
7. S. Liu and P. Han, "Research of the photoelectric tracking and pointing platform based on the servo control system," *J. Aerosp. Technol. Manage.* **11**(1), e1419 (2019).
8. Y. Liu et al., "Control technology of stable gaze scanning based on airborne platform," *Opt. Eng.* **60**(11), 11610201–11610214 (2021).
9. D. H. Klyde et al., "Piloted simulation evaluation of tracking mission task elements for the assessment of high-speed handling qualities," *J. Am. Helicopter Soc.* **65**(3), (2020).
10. Y. Z. Tang, "Development status and trend of foreign airborne optoelectronic pods," *Cloud Light Technol.* **53**(1), 10–17 (2021).
11. B. Everstine, "Infrared IRST pod reaches IOC On USAF F-15Cs," *Aerosp. Daily Defense Rep.* **279**(28), 4–5 (2022).
12. G. L. Jiang, Z. N. Xu, and K. Y. He, "Lightweight design and analysis of a microphotoelectric pod structure," *Mach. Des.* **039**(001), 13–16 (2022).
13. W. Z. Kai, Q. J. Zhang, and S. Li, "Research on multi axis parallelism calibration of space photoelectric tracking and aiming system," *China Opt.* **14**(3), 625–633 (2021).
14. H. Zhang et al., "Design and implementation of electronic image stabilization system based on dual-core DSP," *Proc. Comput. Sci.* **4**(4), 598–607 (2011).

15. Z. Liu et al., "Investigation on the perturbation characteristics and compound axis control for submarine-borne servo system," *Acta Armamentarii* **5**(2), 215–224 (2019).
16. X. S. Shi, W. T. Song, and D. Guo, "Selectively visualizing the hidden modes in random lasers for secure communication," *Laser Photonics Rev.* **15**(10), 2100295 (2021).
17. Q. H. Mo, J. B. Yu, and C. Chen, "Highly efficient and ultra-broadband yellow emission of lead-free antimony halide toward white light-emitting diodes and visible light communication," *Laser Photonics Rev.* **16**(10), 2100600 (2022).
18. Z. W. Sun, M. Z. Du, and R. L. Xu, "Wireless communication utilizing berry-phase carriers," *Laser Photonics Rev.* **16**(4), 2100432 (2022).
19. J. You, Y. K. Luo, and J. Yang, "Hybrid/integrated silicon photonics based on 2D materials in optical communication nanosystems," *Laser Photonics Rev.* **14**(12), 2000239 (2020).
20. Y. Song and S. F. Tong, "Sub micro radian fine tracking system optimization design," in *Int. Conf. Optoelectron. & Microelectron.*, IEEE, pp. 323–327 (2012).
21. F. Wang, Y. F. Gao, and L. I. Qing-Jun, "A vertex tracking technique for airborne photoelectric equipment," *Mod. Electron. Tech.* **035**(017), 144–149 (2012).
22. S. Yoon, S. Park, and Y. Kim, "Circular motion guidance law for coordinated standoff tracking of a moving target," *IEEE Trans. Aerosp. Electron. Syst.* **49**(4), 2440–2462 (2013).
23. K. Yan et al., "INS-aided tracking with FFT frequency discriminator for weak GPS signal under dynamic environments," *GPS Solutions* **21**(3), 917–926 (2017).
24. L. F. Yang and W. H. Chang, "Synchronization of twin-gyro precession under cross-coupled adaptive feedforward control," *J. Guidance Control Dyn.* **19**(3), 534–539 (2012).
25. J. Waldmann, "Feedforward ins aiding: an investigation of maneuvers for in-flight alignment," *Sba: Controle Automação Soc. Brasileira de Automat.* **18**(4), 459–470 (2007).
26. Z. Deng et al., "Switching method for long-term inertial navigation system based on switched control," *J. Navigation* **72**(5), 1315–1330 (2019).
27. D. Lyu et al., "Landmark-based inertial navigation system for autonomous navigation of missile platform," *Sensors* **20**(11), 3083–3091 (2020).
28. S. H. Chen and X. C. Mao, "Research and implementation of Beidou-3 satellite multi-band signal acquisition and tracking method," *J. Shanghai Jiaotong Univ.* **24**(05), 29–36 (2019).
29. L. Chen et al., "Repair of spline shaft by laser-cladding coarse TiC reinforced Ni-based coating: process, microstructure and properties," *Ceram. Int.* **47**(21), 30113–30128 (2021).

Yang Liu received his BS degree from the School of Optoelectronic Engineering Technology, Changchun University of Science and Technology, Changchun, China, in 2016 and his PhD in 2019. Currently, he is a lecturer at Changchun University of Science and Technology and a postdoctoral employee of Changchun Institute of Optics and Mechanics, Chinese Academy of Sciences. His research interests include optical communication and the field of coherent detection.

Zhe An received his BS degree from the School of Changchun University of Science and Technology, Jilin, China, in 2016. She received her PhD in 2019 and is now a lecturer at Changchun Institute of Engineering. Her research focus is image recognition and tracking.

Yansong Song received his PhD from the Department of Optical Engineering, Changchun University of Science and Technology, Jilin, China. He is currently an associate professor in the Institute of Space Optics and Electronics technology. His current research interests are in the areas of servo-control.

Yan Dong received his PhD from the Department of Electronic Information, Changchun Institute of Optics, Fine Mechanics and Physics, Chinese Academy of Sciences, Jilin, China. He is currently an associate professor in the Institute of Space Optics and Electronics Technology. His current research interests are in the areas of servo-control.

Ye Gu received the master's degree from Changchun University of Technology, Jilin, China. He is currently pursuing his PhD in Changchun University of Science and Technology. His research interests include the communication engineering and automatic control.